Heat Risk Mapping of Vulnerable Population using Multi-temporal Satellite Observations in Nakhon Ratchasima Province, Thailand

Lhapawong K. *, Kitratporn N., Kaewmesri P., Pleebut M., Chaikampa A., and Sukawattanavijit C.

Geo-Informatics and Space Technology Development Agency (GISTDA), Bangkok, Thailand

Kulapach@gistda.or.th (*Corresponding author's email only)

***Abstract*:** *The continuous rise in global average temperatures is increasingly impacting public health, particularly in terms of heat exposure. Thailand faces heatwaves annually, with Nakhon Ratchasima province being one of province classified by the Department of Health as a high-risk zone for heat-related hazards. This study examines trends in heat index changes based on land surface temperature (LST) measurements from the Terra/Aqua MODIS satellite system, covering both daytime and nighttime from 2013 to 2023 and analyze the potential impact of land cover and El Niño Southern Oscillation. A bivariate map of heat index using the Urban Thermal Field Variability Index (UTFVI) and vulnerable population aged 60 and above in Nakhon Ratchasima province was developed for 2023 summer months. The study found that UTFVI during daytime reached its peak in February and March, with a decline in April. For nighttime, the UTFVI was the highest in April and May. Areas with high nighttime UTFVI values were predominantly concentrated in urban zones with high population density. The top three districts exhibiting both high UTFVI values and large vulnerable populations during both day and night were Dan Khun Thot, Non Sung, and Phimai. Meanwhile, the districts with the lowest risk are Wang Nam Khiao, Khon Buri, and Soeng Sang, which aligns with land-use changes such as an increase in forested areas, a decrease in grasslands, and a reduction in agricultural areas. The overall changes in provincial average UTFVI were similar with the pattern of ENSO. This data can be applied to analyze priority areas and support effective planning to mitigate heat-related health risks for vulnerable populations.*

Keywords: Land surface temperature, Vulnerability, Time-series analysis, Public health, MODIS

Introduction

Heat is a threat to public health, especially as temperature is expected to continuously increase due to climate change. Heat hazards negatively impact health, leading to diseases and deaths from conditions such as heat exhaustion, heatstroke, cardiovascular disease, respiratory diseases, kidney disease, and even mental health issues. Key vulnerable groups severely affected by extreme heat include children, the elderly, individuals with pre-existing medical conditions, pregnant women, those exercising outdoors, and other at-risk populations (Department of Health, 2023). Assessing the risk posed by heat hazards to vulnerable populations is therefore essential.

Vulnerable groups to heat hazards vary, with the elderly population being one of the rapidly growing groups. The United Nations does not set a specific age for defining the elderly, but a guide by the World Health Organization generally recognizes individuals aged 60 and

above to be under elderly group (Gray et al., 2023). According to the Population and Housing Census in 2000, only 9.5% of the total population in Thailand were aged 60 years or older. However, projections for the future indicate that by 2030, the country is expected to reach the status of an "Aged Society," meaning that more than 20% of the population will be 60 years or older (National Statistical Office, 2021).

Environmental data can be studied through various methods, and satellite data is widely accepted due to its ability to cover large areas and provide continuous information over multiple years. Land surface temperature (LST) data from the Moderate Resolution Imaging Spectroradiometer (MODIS) sensor onboard Terra and Aqua satellites, providing observation with a spatial resolution of 1 km, is one of the most widely used datasets. The LST data from MODIS has been used for long-term global temperature trend studies. (Phan, T. N., & Kappas, M. (2018).) analyzed academic articles related to MODIS LST published during 2009 to 2018 and found that the publications have increased annually, covering 19 fields of study ranges from environmental sciences, agriculture, and biology to social sciences and medicine. This indicates the various applications of MODIS LST data. Key research topics which include urban heat islands (UHI), air temperature estimation and mapping, soil moisture evaluation, water evaporation estimates, and drought monitoring, are the most popular utilization of LST dataset from MODIS.

The urban heat island phenomenon has been analyzed using MODIS data and the simplified urban-extent (SUE) method, covering 9,500 cities over 15 years and found UHI to be 0.85°C during the day and 0.55°C at night, with variations in tropical, temperate, and cold regions (T. Chakraborty & X. Lee, 2019). This study indicated that vegetation significantly influenced UHI changes. Additionally, a study on UHI and the Urban Thermal Field Variability Index (UTFVI) was conducted to compare surface temperature changes with land use changes and found that green spaces declined by over 50% over 21 years, leading to UTFVI being classified as "Worst" (Amindin A et al., 2021).

Nakhon Ratchasima is one of the provinces most severely affected by heat hazards and is classified as a high-risk zone for heat-related dangers by the Department of Health. According to the official population registration data from the Department of Provincial Administration, Ministry of Interior (Department of Provincial Administration, 2024), over the past 10 years (from 2013 to 2023), the number of vulnerable individuals aged 60 and above increased from 271,571 to 398,331.

Therefore, this study aims to analyze trends of the heat index derived from satellite data and to explore the relationship between the heat index and environmental factors, including land use changes and El Niño Southern Oscillation (ENSO). Additionally, the study mapped the heat index and the elderly vulnerable population using bivariate choropleth, with the objective of developing a heat risk map for vulnerable populations in Nakhon Ratchasima province.

Data and Methodology

a. Study area:

Nakhon Ratchasima is a province located in the northeastern region of Thailand, situated on the Khorat Plateau at a latitude of 15 degrees north and a longitude of 102 degrees east, with an elevation of 187 meters above sea level. Its total area is 20,493.964 km^2, accounting for 12.12% of the northeastern region. The province comprises of 32 district and is bordered to the north by Chaiyaphum and Khon Kaen provinces, to the south by Prachinburi, Nakhon Nayok, and Sa Kaeo provinces, to the east by Buriram and Khon Kaen provinces, and to the west by Saraburi and Lopburi provinces (Department of Provincial Administration, 2024) (Figure 1). The population of Nakhon Ratchasima totals 2,625,794 people, comprising of 1,286,634 males and 1,339,160 females, with 531,112 elderly individuals aged 60 and above. Based on the 2019 land use data, the area consists of 1,657.49 $km^2$of urban and built-up land, 14,148.73 km^2 of agricultural land, 3,528.77 km^2 of forest, 529.69 km^2 of water bodies, 832.12 km^2 of miscellaneous land, 29.31 km^2 of lowland rice fields, and 2.30 km^2 of lowland sugarcane fields (Department of Provincial Administration, 2024).

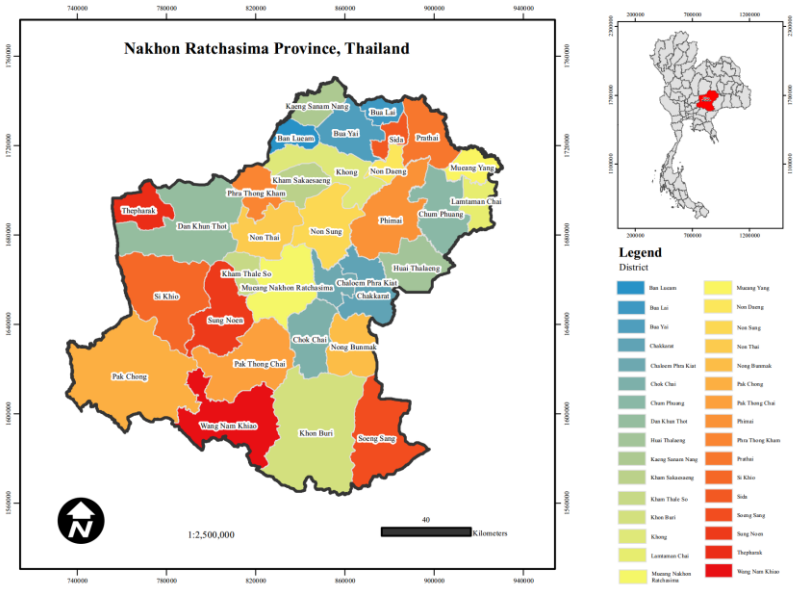

Figure 1 : Study area Nakorn Ratchasima Province, Thailand

b. Data:

Land Surface Temperature

The Land Surface Temperature (LST) data is obtained from the MODIS sensor onboard Terra and Aqua satellite. The LST product is provided in MOD11_L2 LST dataset which monitors and analyzes the Earth's surface temperature during both daytime and nighttime. The data is processed using the Generalized Split-Window Algorithm, which calculates surface temperature from radiation data across different frequency bands. The resulting information can be utilized for studying surface temperature changes at both spatial and temporal scales. The MODIS L2 LST product consists of nine scientific datasets (SDSs) as shown in Table 1: LST, QC, Error_LST, Emis_31, Emis_32, View_angle, View_time, Latitude, and Longitude. The first seven SDSs are at a 1-kilometer pixel resolution, while Latitude and Longitude have a coarser resolution of 5 lines x 5 samples. These geographic data correspond to the center pixels in the LST dataset. The mapping between geographic data and the scientific data sets is managed through StructMetadata.0, created using the HDF-EOS SDPTK toolkit during data processing. This mapping utilizes an offset of 2 and an increment of 5, aligning geographic elements with the LST data structure (USGS, n.d.).

This study obtained the MOD11A1 product via the Google Earth Engine platform. Both daily daytime and nighttime LST data with spatial resolution of 1x1 km^2 were collected and composited into monthly datasets spanning the period from 2013 to 2023 for the study area.

Table1. The Scientific data sets in the MOD11_L2 product (USGS, n.d.)

SDS name	Name	Number Type	Unit	Valid Rage	Fill Value	Scale factor	add offset
LST	Land-surface temperature	uint16	K	7500-65535	0	0.02	0.00
QC	Quality control for LST and emissivity	uint16	none	0-65535	0	NA	NA
Error_LST	Land-surface temperature error	uint8	K	1-255	0	0.04	0
Emis_31	Band 31 emissivity	uint8	none	1-255	0	0.002	0.49

SDS name	Name	Number Type	Unit	Valid Rage	Fill Value	Scale factor	add offset
Emis_32	Band 32 emissivity	uint16	none	1-255	0	0.002	0.49
View_angle	zenith angle of MODIS viewing at the pixel	uint8	deg	0-180	0	0.5	0
View_time	Time* of Land-surface Temperature observation (* as local solar time)	Uint8	hrs	0-240	0	0.1	0
Latitude	Latitude of every 5 scan lines and 5 pixels	float32	degree	-90.0 to 90.0	-999.9	NA	NA
Longitude	Longitude of every 5 scan lines and 5 pixels	float32	degree	-180.0 to 180.0	-999.9	NA	NA

Satellite-derived Heat Index

The urban heat phenomenon describes the elevated temperature in urban areas compared to rural surroundings, often accompanied by higher pollution levels (Amindin et al., 2023; Cevik & Cetin., 2023; Abir et al., 2021) and adverse health effects. From LST, this study calculated two commonly used heat indices, namely the Urban Heat Index (UHI) and the Urban Thermal Field Variance Index (UTFVI).

The UHI is calculated based on the following equation following previous studies (Amindin et al., 2023; Cevik & Cetin., 2023; Abir et al., 2021).

$$UHI = (T_i - T_{mean}) / T_{sd}$$

Where:

T_i is the land surface temperature at a given pixel

T_{mean} is the average land surface temperature in the study area

T_{sd} is the standard deviation of land surface temperature in the study area

The UTFVI is another widely adopted measure used to assess the effects of urban heat phenomenon, particularly in terms of thermal comfort levels in urban environments (Amindin et al., 2023; Cevik & Cetin., 2023; Abir et al., 2021). The UTFVI is calculated based on a specific formula below and can be classified using the ranges shown in Table 2., which helps in comparing different areas' thermal conditions and identifying areas with elevated discomfort levels.

$$UTFVI = (T_i - T_{mean}) / T_i$$

Where:

T_i is the land surface temperature at a given pixel

T_{mean} is the average land surface temperature in the study area

Table 2. UTFVI range (Amindin et al., 2023; Cevik & Cetin., 2023)

UTFVI Range	UTFVI Class
< 0.00	Best
0.00 - 0.005	Better
0.005 - 0.010	Normal
0.010 - 0.015	Bad
0.015 - 0.020	Worse
> 0.020	Worst

Land Cover Classification

The MODIS Land Cover Type Product (MCD12Q1) offers global land cover maps at a 500-meter resolution on an annual basis, spanning from 2001 to the present through Google Earth Engine. The analysis utilized the MCD12Q LC_Type1 classes (Table 3.), which are derived from the IGBP classification system consisting of 18 distinct classes (LP DAAC., 2021; Hankui & David., 2017). For this study, these 18 land cover classes were reclassified into 6 broader categories to simplify the analysis. (Table 4.)

Table 3. Global maps of land cover

LULC Class	Description	Source
MCD12Q LC_Type1	Global maps of land cover at annual time steps and 500-m spatial resolution for 2001-present	https://developers.google.com/earth-engine/datasets/catalog/MODIS_061_MCD12Q1

Table 4. Land Cover Reclassify (Bashir et al., 2022)

LULC Class	Name	Description
Forest	Evergreen Broadleaf Forests	Dominated by evergreen broadleaf and palmate trees (canopy >2m). Tree cover >60%.
	Deciduous Broadleaf Forests	Dominated by deciduous broadleaf trees (canopy >2m). Tree cover >60%.
	Mixed Forests	Dominated by neither deciduous nor evergreen (40-60% of each) tree type (canopy >2m). Tree cover >60%.
Grasslands	Closed Shrublands	Dominated by herbaceous annuals (<2m).
	Open Shrublands	Dominated by woody perennials (1-2m height) >60% cover.
	Woody Savannas	Dominated by woody perennials (1-2m height) 10-60% cover.
	Savannas	Tree cover 30-60% (canopy >2m).
	Grasslands	Dominated by herbaceous annuals (<2m).
Croplands	Croplands	At least 60% of area is cultivated cropland.
	Cropland/Natural Vegetation Mosaics	Mosaics of small-scale cultivation 40-60% with natural tree, shrub, or herbaceous vegetation.
Urban and Build-up Lands	Urban and Built-up Lands	At least 30% impervious surface area including building materials, asphalt, and vehicles.
Water bodies	Permanent Wetlands	Permanently inundated lands with 30-60% water cover and >10% vegetated cover.
	Water Bodies	Atleast 60% of area is covered by permanent water bodies.
Barren	Barren	At least 60% of area is non-vegetated barren (sand, rock, soil) areas with less than 10% vegetation.

Valuable populations

Figure 2 shows data on vulnerable populations from the Department of Provincial Administration, Ministry of Interior (Department of Health, 2023), The data is based on the

household registration in Nakhon Ratchasima Province. This data includes individuals aged 60 and above for each district, covering the years 2013 and 2023.

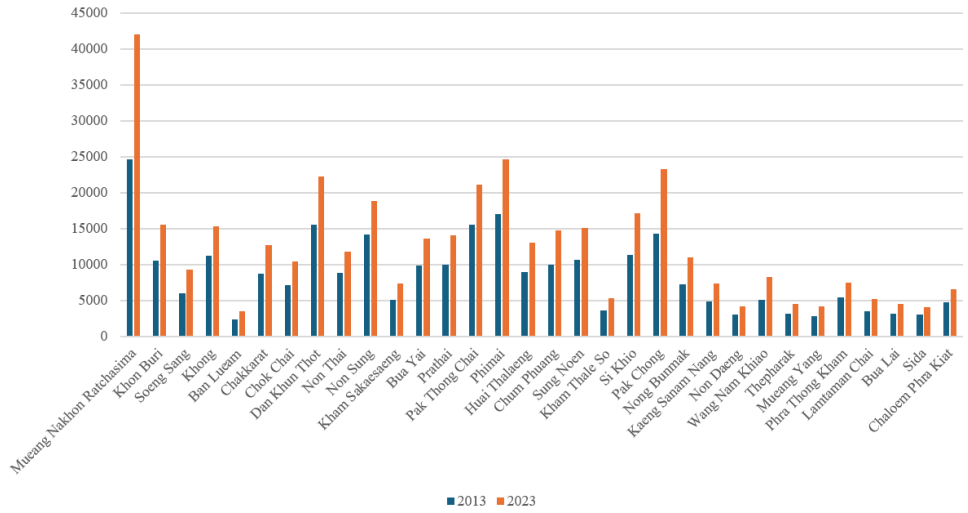

Figure 2 : Population in Nakhon Ratchasima Province

c. Research Methodology:

Figure 3 illustrates the overall flow of this study. Satellite-based heat indicators were calculated. The correlation coefficient between three heat indicators, namely LST, UHI, and UTFVI was analyzed. The UTFVI was chosen for trend and change analysis in relation to land cover change and the El Niño-Southern Oscillation (ENSO) phenomena. The UTFVI during the summer months, February to May, of 2023 and the vulnerability based on elderly population in each district of the same year were mapped to priority area with highest potential risk.

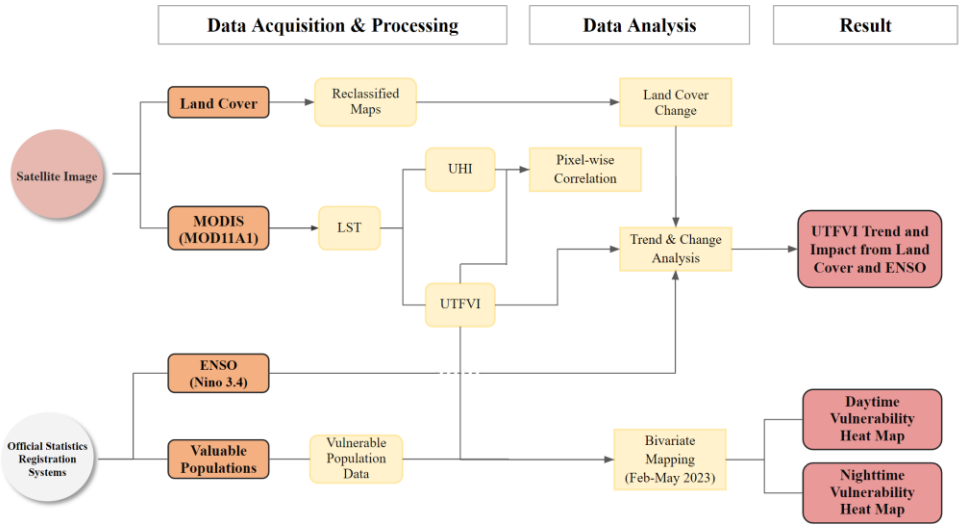

Figure 3 : Overall methodology used in this study

Correlation Analysis Among Heat Indices

Analyzing the relationship between LST, UHI and UTFVI helps to understand the connection between the urban heat island phenomenon and surface heat. This analysis uses pixel-wise correlation to determine, with the correlation coefficient measuring the strength of the association between variables. The coefficient ranges from -1 to 1: a positive value indicates a direct (same direction) relationship, while a negative value indicates an inverse (opposite direction) relationship (Angsuchoti., 2024; Silpakit., 2024). The formula is as follows:

$$r = \frac{\sum(X - \bar{X})(Y - \bar{Y})}{\sqrt{\sum(X - \bar{X})^2 \sum(Y - \bar{Y})^2}}$$

Trend and Change Analysis of Heat Index

The analysis of data trends is conducted to examine the directional changes in data over a given period. It is a fundamental tool in forecasting, allowing researchers to project the future trajectory of variables based on historical data (Angsuchoti., 2024; Silpakit., 2024). This process involves identifying whether the data exhibits increasing or decreasing patterns, which is crucial for understanding historical shifts and making informed predictions about future behavior. The trend is typically quantified through the slope of the data fitted using linear regression calculated over a period. In this study, the trend of each summer month was calculated over an 11-year period from 2013 to 2023. A positive slope suggests an upward trend, indicating a likely increase in future data values. In contrast, a negative slope signals a downward trend, implying a potential decline in future observations. In additional, the change of heat index, specifically the UTFVI, was compared to the change in land cover and ENSO phenomena to understand potential driver of the shift and variation in UTFVI.

Heat Index and Vulnerability Mapping

To combine the heat index characteristic with ranges of vulnerable population over the age of 60 years old, bivariate choropleth mapping was performed. This approach allows to visualize, among geographical unit, two key variables simultaneously. Biesecker et al. (2020) emphasized the importance of bivariate choropleth mapping in public health which helps in prioritizing the areas with greatest needs and guiding the allocation of resources. This study generated 3x3 dimension with equal interval between UTFVI and vulnerable elderly population which allows the high, medium, and low characteristics of each variable to intersectThe mapping was performed using UTFVI from each summer month in 2023, specifically February

to May, and the vulnerable population in 2023. Both variables were normalized with min-max normalization prior to mapping.

Results and Discussion

a. Analysis of Heat Index :

The Correlation of Heat Indices at the Pixel Level

The correlation coefficient among LST, UHI, and UTFVI calculated from 2013 to 2023 is shown in Figure 4. The result indicates similar characteristics of UHI and UTFVI with correlation coefficient very close to 1. In addition, both correlation coefficient of LST-UHI and LST-UTFVI were positive in most locations. The urban, large waterbody, and forested areas showed slightly lower correlation between LST and the two heat indices. Since UHI and UTFVI showed close relationship, this study chose UTFVI for further analysis because it is an indicator of the severity of the impact of the urban heat island phenomenon and it provides severity ranking.

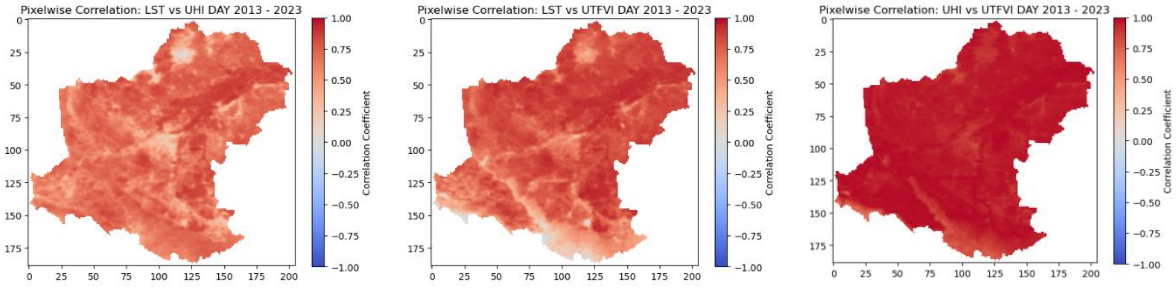

Figure 4 : The Correlation Between Heat Index (LST) at the Pixel Level

Trends in Heat Index from Satellite Data

Based on the trend analysis of an 11-year period during summer months, the majority of the areas experienced a decreasing trend for the daytime as shown in Figure 5(a). There was a noticeable increase in the UTFVI index during March compared to other months, implying a rise in temperature during this time over the years. Interestingly, the UTFVI showed a large area with decreasing trend in April which suggests that despite the ongoing summer heat, the temperature might not rise as dramatically as in March. Possible explanations could include seasonal weather patterns, such as increased cloud cover, rainfall, or vegetation regrowth in certain areas that help mitigate extreme heat.

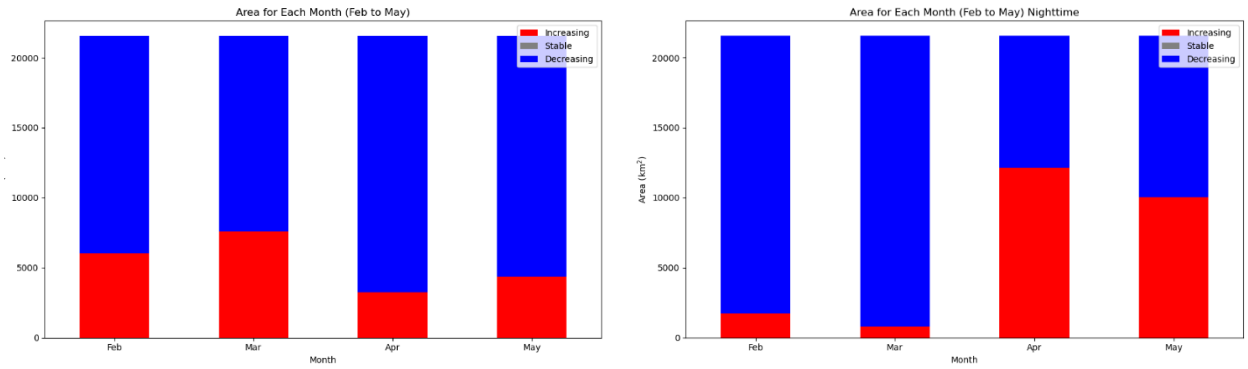

(a) (b)

Figure 5 : Area of increasing and decreasing UTFVI for day (a) and night (b) from 2013 to 2023

During the nighttime the heat index shows a large increase in April and May compared to the other two months as shown in Figure 5(b). This indicated that nighttime temperatures are getting warmer later in the season. This may be the result of direct increase of nighttime temperature and the effect in which the ground retains more heat from daytime and releases slowly at night. Such trends can be associated with the urban heat island effect, where built-up areas retain more heat compared to rural surroundings, especially as the season progresses.

The percentage of areas based on the severity levels of the UTFVI can be categorized as shown in Figure 6. For the daytime (Figure 6(a)) in March, April, and May, it can be observed that the "Worst" category in 2023 has significantly decreased compared to 2013. At the same time, the "Best" category in 2023 has shown an increase compared to 2013. Despite this improvement of the daytime UTFVI, roughly 50 percent of the province areas remain under “Bad”, “Worse”, and “Worst” classification. Meanwhile, nighttime UTFVI, shown in Figure 6(b), illustrates an interesting pattern with worsen classification of the UTFVI in April and May. Although the area classified as "Best" increased compared to 2013 in February and March, opposite situation was seen for April where more area experienced increasing “Bad” UTFVI classification.

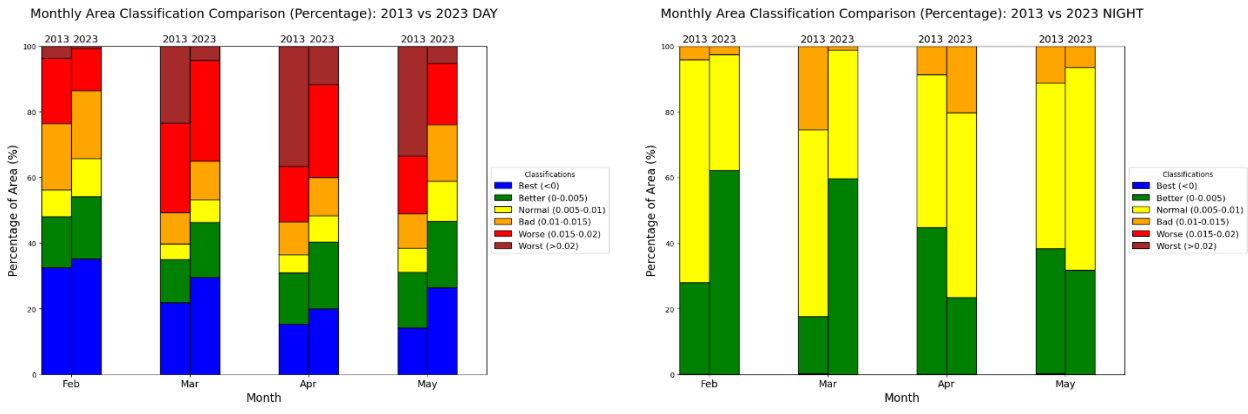

(a) (b)

Figure 6 : The percentage of UTFVI classification for day (a) and night (b) for 2013 and 2023

In comparing daytime and nighttime UTFVI, daytime temperatures generally reflect higher heat due to solar radiation and urban heat island effects, with categories such as "Worse" and "Worst" indicating extreme heat conditions. Nighttime temperatures typically cool down as shown in lower UTFVI classes. From February to May, the analysis shows that daytime temperatures in 2023 improved notably compared to 2013. Specifically, in February and March, there was an increase in areas classified as "Best" and "Better," which also in turn improved cooling effects at night. However, April and May saw a decline in these cooler categories and an increase in "Bad" classifications, indicating reduced nighttime cooling efficiency and higher temperatures.

These changes have significant implications for health and vulnerable populations. Higher nighttime temperatures can exacerbate health issues, particularly for those with pre-existing conditions, the elderly, and low-income individuals who may lack adequate cooling resources. Improved daytime conditions may help mitigate some heat-related risks, but persistent elevated nighttime temperatures can still pose serious health risks, highlighting the need for ongoing adaptation and support strategies.

Change of Heat Index and the Impact of Land Cover

Figure 7 shows the maps of land cover in 2013 and 2022 on which the distribution of land cover did not change significantly. However, the total areas change for each land cover class can be observed as listed in Table 6. Comparing land cover between 2013 and 2022 found an increase in forested areas which indicated by more green regions, likely contributes to improved environmental conditions. Forests generally help reduce surface temperatures by providing shade and promoting evapotranspiration, which can mitigate urban heat. Conversely, the decrease in croplands (yellow) and grasslands (light green) between 2013 and 2022 may also influence the heat patterns. Croplands and grasslands can have varied effects on heat retention, depending on the crop types and density of vegetation cover.

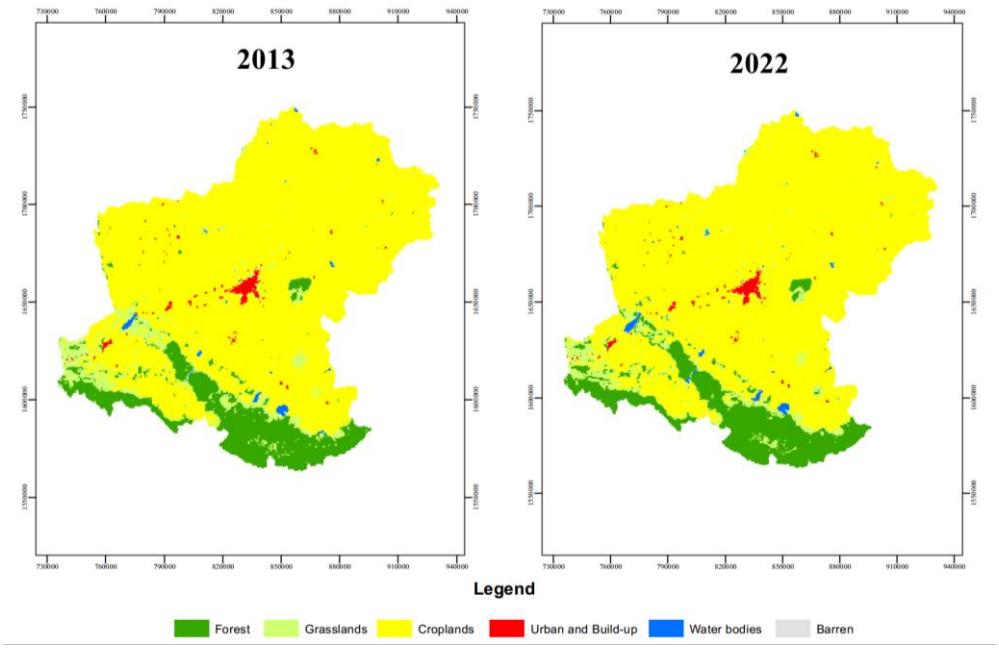

Figure 7 : Land Use and Land Cover in 2013 and 2022

Table5. Land Cover Change

Class	2013 Area (km^2)	2022 Area (km^2)	Area (km^2)
Forest	2491.5	2628	136.5 (Increase)
Grasslands	1490.75	1401	-89.75 (Decrease)
Croplands	17445.5	17381.75	-63.75 (Decrease)
Urban and Build-up	201	201	0 (Stable)
Water bodies	88.75	106.75	18 (Increase)
Barren	1.25	0.25	-1 (Decrease)

Figure 8 illustrates the UTFVI classification during April, which is the peak of summer month in 2013 (left) and 2023 (right) for daytime (top) and nighttime (bottom). For daytime UTFVI, an improvement in UTFVI values from 2013 to 2023 was observed, particularly in regions where the index changes from "Worst" to lighter shades. These improvements may be related to the increase in forest areas and reduction in croplands, as these land cover changes generally lead to cooler surface temperatures and healthier environmental conditions. Additionally, the agriculture activities likely changed which led to the improvement of UTFVI. The stability in urban and build-up areas reflected in the UTFVI maps, where some urban regions continue to experience the "Worst" environmental condition in both 2013 and 2023. Urban areas tend to trap heat, leading to higher temperatures and poorer environmental quality.

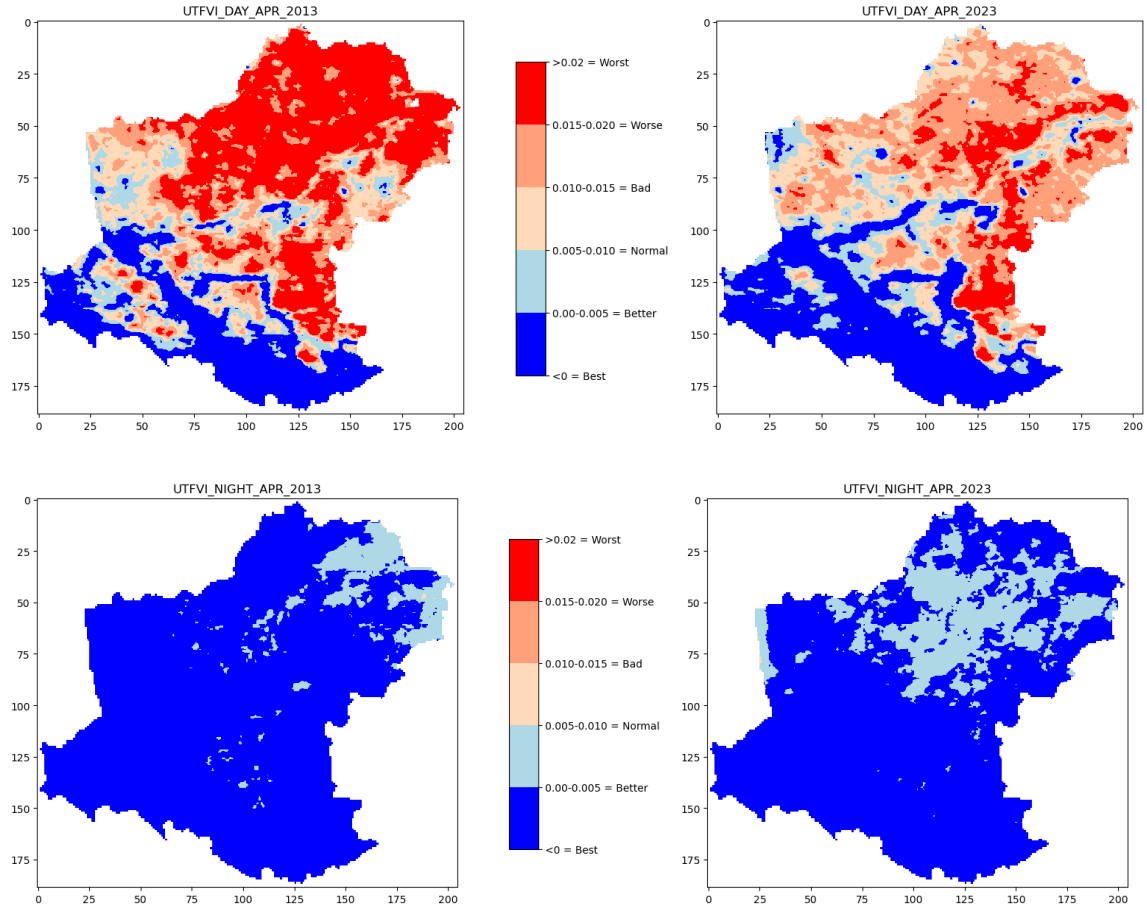

Figure 8 : Compare between Daytime and Nighttime (April, 2023)

The changes in land use and land cover, particularly the increase in forest cover and the decrease in cropland areas, are likely contributing to the improved UTFVI conditions in certain areas. This demonstrates how land management and natural changes over time can directly influence the urban thermal environment and overall environmental health. The connection between the two image sets highlights the importance of sustainable land use planning in mitigating the negative effects of urban heat and environmental degradation.

Change of Heat Index and the Impact of the ENSO Phenomenon

Over the five-year period, UTFVI values displayed minimal variation after 2020 onward (Figure 9). Starting at 0.0069 in 2019, the index decreased to 0.0044 in 2020 and remained relatively stable from 2020 to 2023, fluctuating between 0.0041 and 0.0048. This stability suggests that thermal variance in urban areas was largely consistent during these years and did not experience significant changes. In contrast, the Nino3.4 index, which tracks sea surface temperature anomalies and serves as an indicator of El Niño and La Niña events, exhibited notable fluctuations. In 2019, the index was relatively high (0.6725), signifying a warm phase associated with El Niño conditions. However, in the following years, the index dropped

significantly, reaching negative values in 2021 (-0.745) and 2022 (-1.02), indicating a transition to La Niña. By 2023, Nino3.4 had returned to near-neutral conditions (0.0075), suggesting a stabilization of the climate.

The analysis reveals a possible indirect correlation between large-scale climate phenomena, such as El Niño and La Niña, and urban thermal dynamics. Specifically, the cooler La Niña phases in 2021 and 2022 were associated with marginally lower UTFVI values, potentially suggesting that global cooling trends during La Niña may reduce urban thermal intensities. However, the observed relationship is not conclusive, and further research with extended datasets is necessary to establish any causal link. This finding underscores the importance of continuous monitoring to better understand the relationship between global climate systems and localized urban thermal patterns.

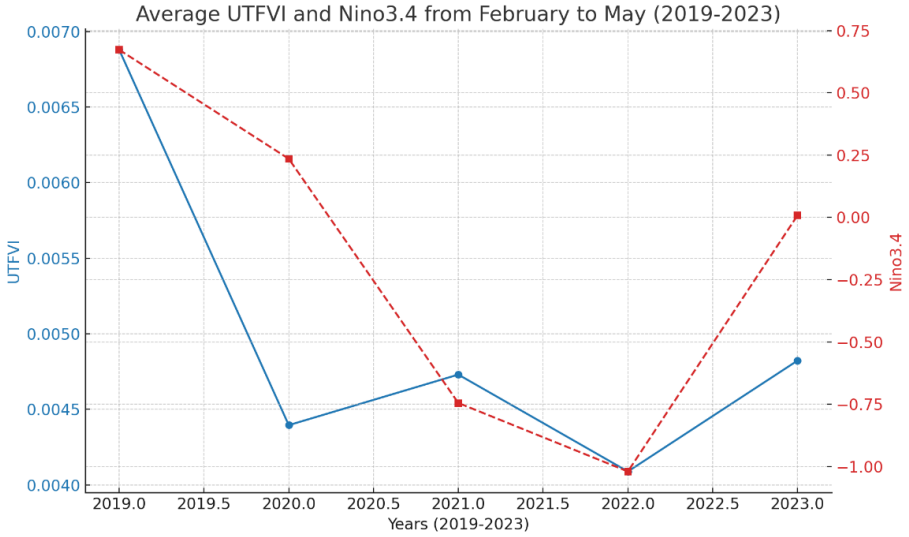

Figure 9 : the average UTFVI and Nino3.4 data from February to May for the years 2019 to 2023. The blue line indicates the UTFVI, while the red dashed line represents Nino3.4

b. Heat Risk Map for Vulnerable Populations :

Mapping Between UTFVI and Vulnerability Population (Daytime)

The Figure 10 shows the analysis of the bivariate map between the UTFVI and the vulnerable population during the daytime in 2023 from February to April. Three districts, namely Dan Khun Thot, Non Sung, and Phimai, shows prominent high-high classification which indicates high UTFVI and high vulnerability across February to March. Conversely, the districts with the consistent low-low classification were Wang Nam Khiao, Khon Buri, and Soeng Sang. Meanwhile May illustrated different pattern with Mueang Nakhon Ratchasima District experience high UTFVI shifting the classification from low-high to

high-high. The other top district in May were Non Sung and Phimai, while newly identified low-low districtwas Thepharak District. Table x lists the top and bottom three districts.

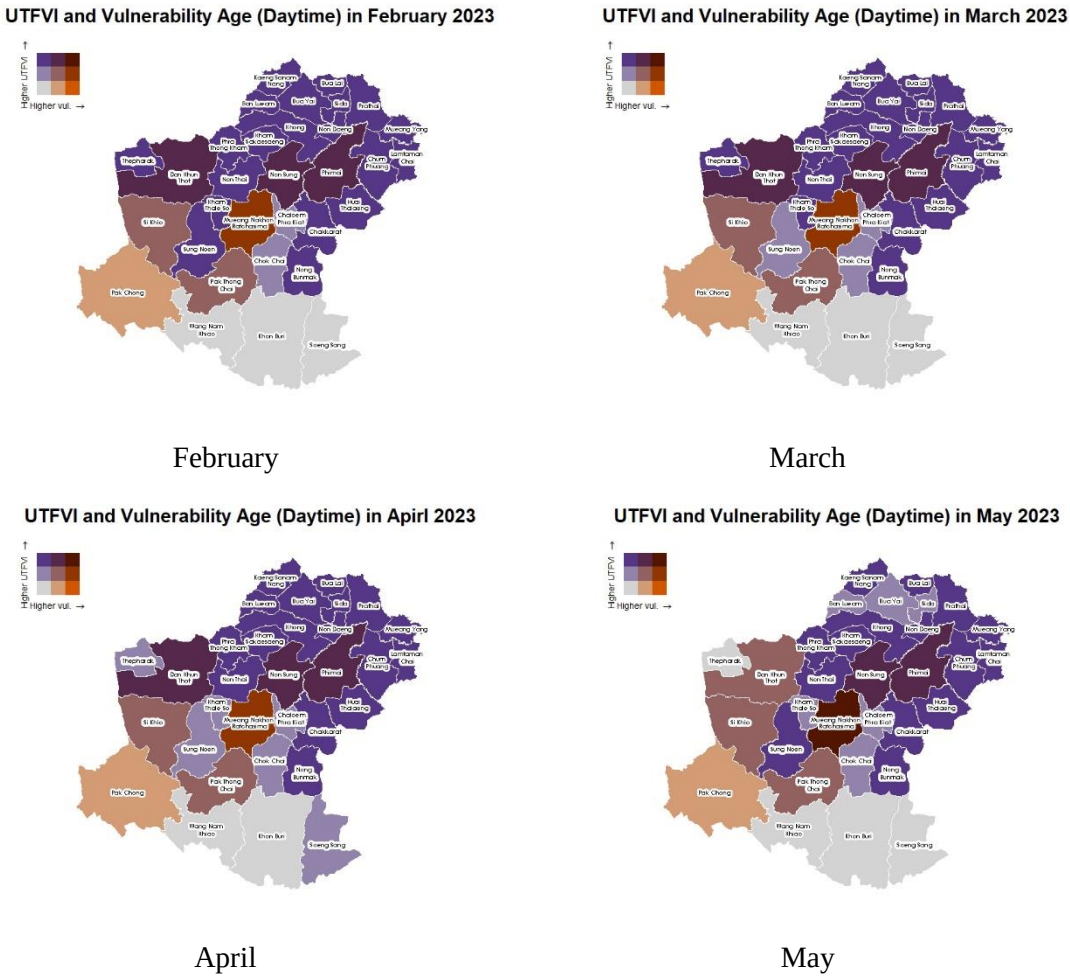

Figure.10 : Bivariate map of UTFVI and Vulnerable Population (Daytime) in 2023

Table 6. Top and Bottom Ranked Districts by Population and UTFVI Risk (Daytime)

District	Populations		UTFVI Range Risks (Daytime)
	2013	2023	
Top 3 Rankings			
1. Dan Khun Thot	15,553	22,217	High
2. Non Sung	14,187	18,869	High
3. Phimai	17,019	24,660	High
Bottom 3 Rankings			
1. Wang Nam Khiao	5,104	8,258	Low
2. Khon buri	10,547	15,570	Low
3. Soeng Sang	6,045	9,239	Low

Mapping Between UTFVI and Vulnerability Age (Nighttime)

The Figure 11 shows the analysis of the bivariate map between the UTFVI and the number of vulnerable population groups during the nighttime period in 2023 from February to May. Mueang Nakhon Ratchasima consistently shows high-high classification with high UTFVI and high vulnerability. Its consistently high UTFVI during nighttime is likely related to the urban heat island phenomenon. The increasing development in the district may result in a higher area of accumulated heat due to factors such as heat absorption and storage from construction materials used in the city, as well as a decrease in green areas, or even the heat emissions from people's activities, such as transportation and energy use. Following Mueang Nakhon Ratchasima district, the other two districts persistently illustrate medium-high classification, namely Si Kieo and Pak Thong Chai. On the other hand, Wang Nam Khiao, Khong Buri, and Saeng Sang were grouped in low-low classification. Table x lists the top and bottom three districts.

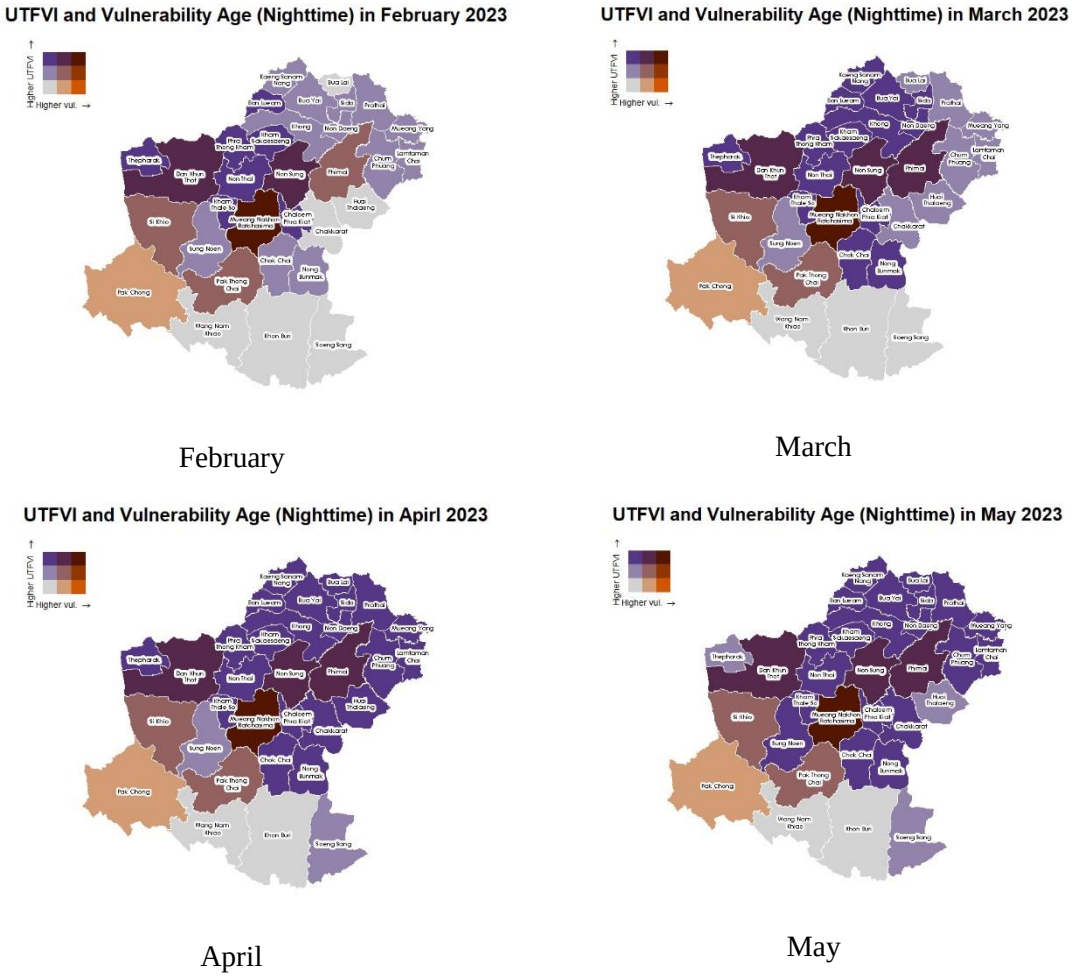

February March

April May

Figure.11 : Bivariate map of UTFVI and Vulnerable Population (Nighttime) in 2023

Table 7 : Top and Bottom Ranked Districts by Population and UTFVI Risk (Nighttime)

District	Populations		UTFVI Range Risks (Nighttime)
	2013	2023	
Top 3 Rankings			
1. Mueang Nakhon Ratchasima	24,599	42,044	High
2 Si Khio	11,327	17.179	Medium
3. Pak Thong Chai	15,509	21,110	Medium
Bottom 3 Rankings			
1. Wang Nam Khiao	5,104	8,258	Low
2. Khon buri	10,547	15,570	Low
3. Soeng Sang	6,045	9,239	Low

Conclusion and Recommendation

The rising trend of temperature, particularly from climate change, will have significant impacts on public health, especially for vulnerable populations aged 60 and above. This research has studied and analyzed the heat index, specifically the Urban Thermal Field Variability Index (UTFVI) both during the daytime and nighttime. From 2013 to 2023, the daytime UTFVI peaked in February and March, while decline in April. The nighttime UTFVI peaked in April and May, with areas of high values often concentrated in urban areas, corresponding to areas with dense populations. Although most of the province experiences decreasing UTFVI trend in the past 11 years, over 50 percent of the areas still listed under “Bad”, “Worse”, and “Worst” category. Additionally, the nighttime UTFVI even worsened in April and May. The drivers of changes and fluctuation in UTFVI were indirectly influenced by the increase in forested areas and the ENSO phenomena, but further investigation is required. When analyzed UTFVI together with the vulnerable populations, three districts with both high UTFVI values and high vulnerable populations for both day and night are Dan Khun Thot District, Non Sung District, and Phimai District. This analysis can be applied to priority heat-risk areas and support effective planning to mitigate heat hazards that could impact the health of vulnerable populations.

References

Abir, F. A., Ahmmed, S., Sarker, S. H., & Fahim, A. U. (2021). Thermal and ecological assessment based on land surface temperature and quantifying multivariate controlling factors in Bogura, Bangladesh. Heliyon, 7(9). https://doi.org/10.1016/j.heliyon.2021.e08012

Amindin, A., Pouyan, S., Pourghasemi, H. R., Yousefi, S., & Tiefenbacher, J. P. (2021). Spatial and temporal analysis of urban heat island using Landsat satellite images. Environmental Science and Pollution Research, 28, 41439-41450. https://doi.org/10.1007/s11356-021-13693-0

Angsuchoti S.(n.d.). Techniques for analyzing the relationship between variables .Retrieved 30 August 2024, from https://www.stou.ac.th/offices/ore/info/cae/uploads/pdf/636366560441132172.pdf

Bashir, A., Nawaz, R., & Shahid, M. (2022). Leveraging cloud-based computing and spatial modeling approaches for land surface temperature disparities in response to land cover change: Evidence from Pakistan. Environmental Monitoring and Assessment, https://doi.org/10.1016/j.rsase.2021.100665

Biesecker, C., Zahnd, W. E., Brandt, H. M., Adams, S. A., & Eberth, J. M. (2020). A Bivariate Mapping Tutorial for Cancer Control Resource Allocation Decisions and Interventions. In Preventing Chronic Disease (Vol. 17). Centers for Disease Control and Prevention (CDC). https://doi.org/10.5888/pcd17.190254

Bureau of Health Impact Assessment, Department of Health, Ministry of Public Health, Report on the Situation and Outcomes of Surveillance and Health Warning Communication from Heat.(2023). Retrieved 9 July 2024, from https://hia.anamai.moph.go.th/web-upload/12xb1c83353535e43f224a05e184d8fd75a/202402/m_magazine/35644/4745/file_download/c4239838ba7712df487d2b896652145f.pdf

Cevik Degerli, B., & Cetin, M. (2023). Evaluation of UTFVI index effect on climate change in terms of urbanization. Environmental Science and Pollution Research, 30(30), 75273-75280. https://doi.org/10.1007/s11356-023-27613-x

Chakraborty, T., & Lee, X. (2019). A simplified urban-extent algorithm to characterize surface urban heat islands on a global scale and examine vegetation control on their spatiotemporal variability. International Journal of Applied Earth Observation and Geoinformation, 74, 269-280. https://doi.org/10.1016/j.jag.2018.09.015

Foody, G.M., Mathur, A., 2006. The use of small training sets containing mixed pixels for accurate hard image classification: training on mixed spectral responses for classification by SVM. Remote Sens. Environ. 103, 179 –189., https://doi.org/10.1016/j.rse.2006.04.001

Gray, R., Phattharawanit, U., Chamchan, C., & Suwannopakao, R. (2013). A New Conceptualization of the Definition of Elderly: A Psychosocial and Health Perspective. Nakhon Pathom: Dueantula Printing Co., Ltd. Retrieved 13 June 2024, from https://ipsr.mahidol.ac.th/wp-content/uploads/2022/03/Report-File-419.pdf

Hankui K. Zhang, David P. Roy ()Using the 500m MODIS land cover product to derive a consistent continental scale 30m Landsat land cover classification, Remote Sensing of Environment,Volume 197, 2017,Pages 15-34, ISSN 0034-4257, https://doi.org/10.1016/j.rse.2017.05.024.

Nakhon Ratchasima Provincial Hall, Department of Provincial Administration, Ministry of Interior.(2024). Retrieved 30 August 2024, from https://www2.nakhonratchasima.go.th/content/general

National Statistical Office.(2021).The Situation of Thai Elderly 2021: Area Disparity. Retrieved 15 August 2024, from https://www.nso.go.th/nsoweb/storage/ebook/2023/20230506145038_72776.pdf

Official Statistics Registration Systems. Department of Provincial Administration, Ministry of Interior. Official Statistics Registration Systems.(2024). Retrieved 21 June 2024, from https://stat.bora.dopa.go.th/stat/statnew/statMenu/newStat/home.php

Phan, T. N., & Kappas, M. (2018). Application of MODIS land surface temperature data: a systematic literature review and analysis. Journal of Applied Remote Sensing, 12(4), 041501-041501. https://doi.org/10.1117/1.JRS.12.041501

Silpakit C.(n.d.). Basic Statistics. Retrieved 30 August 2024, from https://www.rama.mahidol.ac.th/psych/sites/default/files/public/pdf/Conference/Research_conference/57/Basic%20Statistics.pdf

United States Geological Survey, (n.d.). MODIS Land Surface Temperature (LST) Products User's Guide Version 6. Retrieved 18 July 2024, from https://lpdaac.usgs.gov/documents/118/MOD11_User_Guide_V6.pdf

USGS Land Processes Distributed Active Archive Center (LP DAAC). (2021). MCD12 User Guide Version 6.1. Retrieved, from https://lpdaac.usgs.gov/documents/1409/MCD12_User_Guide_V61.pdf